Spectrochimica Acta Part B: Atomic Spectroscopy 198 (2022) 106548

Contents lists available at ScienceDirect

Spectrochimica Acta Part B: Atomic Spectroscopy

journal homepage: www.elsevier.com/locate/sab

Evaluation of different analytical approaches using total reflection X-ray fluorescence systems for multielemental analysis of human tissues with different adipose content

Patrícia M. Carvalho [a], Eva Marguí [b], Aldona Kubala-Kukuś [c,d], Dariusz Banaś [c,d], Jorge Machado [a], Diogo Casal [e], Diogo Pais [e], José Paulo Santos [a], Sofia Pessanha [a,*]

[a] Department of Physics, NOVA School of Science and Technology, NOVA University of Lisbon, Campus Caparica, 2829-516 Caparica, Portugal
[b] Department of Chemistry, Faculty of Sciences, University of Girona, C/M.Aurèlia Capmany, 69, 17003 Girona, Spain
[c] Department of Atomic Physics and Nanophysics, Institute of Physics, Jan Kochanowski University, Uniwersytecka 7, 25-406 Kielce, Poland
[d] Department of Physical Methods, Holy Cross Cancer Center, Artwińskiego 3, 25-734 Kielce, Poland
[e] Department of Anatomy, NOVA Medical School, NOVA University Lisbon, Campo dos Mártires da Pátria 130, 1169-056 Lisboa, Portugal

ARTICLE INFO

Keywords:
TXRF
EDXRF
Multielemental analysis
Human tissues
Sample preparation

ABSTRACT

Elemental content plays an important role in biological processes, and so, the multielemental analysis of human tissue samples is required in biomedical research. Still, the small amount of available biological samples and the adipose content of the samples can be major setbacks for the accurate determination of elemental content.

In this study, we explored the potential of several analytical approaches combined with total reflection X-ray fluorescence spectrometry (TXRF) for multielemental analysis of human tissues with different adipose content (colon, heart, liver, lung, muscle, intestine, skin, stomach, uterus, bladder and aorta). The capabilities and limitations of different sample treatment procedures (suspension and acidic digestion) and two TXRF systems with different anode configurations (Mo and W X-ray tubes) have been evaluated for such purpose. Results showed that for tissues with a higher fat content (e.g., skin, and intestine) the best strategy was the acidic digestion of the sample before TXRF analysis. However, for other tissues, acceptable results were obtained by suspending 20 mg of powdered material in 1 mL of 2 M nitric acid. A further enhancement of the limits of detection and accuracy of the results was achieved if using Mo-TXRF systems, especially for the determination of low Z elements (e.g., K, and Ca) and of elements present at low concentrations (e.g., Cu) in the human tissues.

Finally, results by TXRF analysis were compared with those obtained with μ-EDXRF and ICP-OES, and a good agreement was obtained.

1. Introduction

Elemental content plays an important role in biological processes and an association between the levels of trace elements and the presence of diseases has already been established [1]. For instance, Cu and Zn are cofactors or essential components of nearly 300 enzymes, while Fe is present at the active site of many molecules that are instrumental in biological functions such as oxygen transport, electron transfer, and DNA synthesis [2]. Ca is involved in many cellular processes, such as, apoptosis, gene transcription, and angiogenesis [3], while antioxidant enzymes, such as glutathione peroxidases, require the presence of selenium as an essential cofactor [4].

In order to gauge the elemental content of human tissues, X-ray Fluorescence (XRF) techniques, both in conventional geometry or in total reflection mode (TXRF), have already been tested in research [2,4–11].

The truly multielemental capability of XRF and the possibility to analyze solid samples with a minimum sample treatment are the most important features among the many that have made it a desired analytical tool for element detection in human organ samples. Silva et al. [8] have correlated the presence of trace elements such as Ca, Fe, Cu and Zn in breast tissue with some cancer prognostic factors such as estrogen or progesterone receptors, tumour size and stage, presence of lymph nodes or age and menstrual status of patients presenting both benign and

* Corresponding author.
E-mail address: sofia.pessanha@fct.unl.pt (S. Pessanha).

https://doi.org/10.1016/j.sab.2022.106548
Received 28 April 2022; Received in revised form 29 July 2022; Accepted 15 October 2022
Available online 19 October 2022

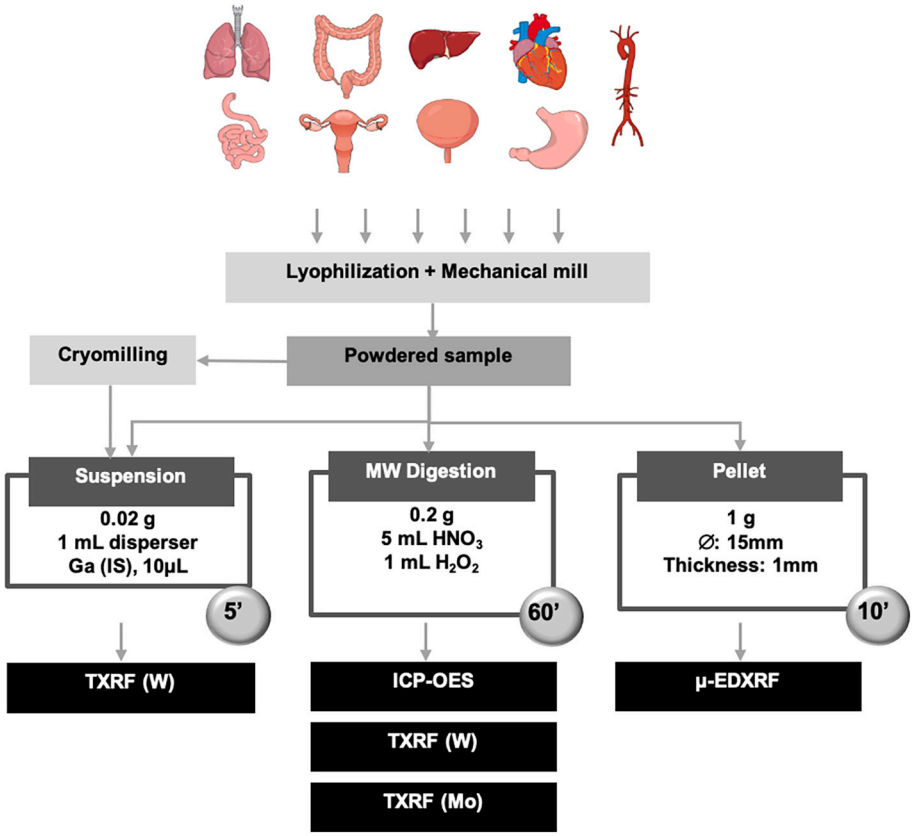

Fig. 1. Scheme of the sample treatment procedures and analytical techniques tested for the analysis of human tissues.

malignant breast tumors. Using a monochromatized 17.44 keV beam and an EDXRF system with 90° geometry for background reduction they found, for instance, a positive correlation between these elements and age and menstrual status. Zaichick & Zaichick [12] also used an EDXRF system to determine and quantify the presence of Br, Fe, Rb, Sr and Zn in prostate tissue and determined a strongly pronounced tendency of age-related exponential increase in Zn as well as an increase in Zn/Fe, Zn/Rb, and Zn/Sr ratios.

One of the main drawbacks of the use of XRF for the analysis of biological samples is the presence of matrix effects and dark matrix estimation for the fundamental parameters approach [13]. A reliable alternative to overcome matrix effects' evaluation could be the use of empirical calibration curves with a set of certified reference materials (CRMs) with a similar matrix to the unknown samples [14] [15]. For instance, this approach was used for the determination of the concentrations of Fe, Cu, and Zn of four sets of paired samples (tumour tissues and surrounding normal tissue) from four cadavers identified with cancer pathology – lung, colon and ovarian carcinoma, and prostate neoplasia [6]. The reference curves used in this work were later improved by establishing a methodology that uses CRMs with different matrices (tissue CRMs + leaves CRMs), but with correction of the intensities with the scattering lines of the X-ray source. This methodology was then applied to lyophilized samples of normal and tumour breast and endometrium tissues [7]. Correcting the net intensities with the scattered peaks from the X-ray source can also be a strategy to overcome the inhomogeneities in sample density and/or thickness. This strategy was also used by Wróbel et al. [10,16] for the establishment of a combined methodology using micro-XRF and TXRF for the imaging of kidney, liver, and spleen samples.

Another analytical approach for multielemental analysis of human tissues in the field of X-rays is the use of TXRF instrumentation. TXRF is a variation of XRF where the primary beam strikes the sample carrier (for example quartz glass reflector), on which sample is deposited, at a small glancing angle, lower than critical angle of the total external X-ray reflection, whose value depends on the sample carrier material and energy of primary X-ray (for 17.44 keV (Mo-Kα) and for quartz sample carrier it is 0.1°, for higher energy the angle is even lower). The detector registering characteristic X-rays emitted from the sample is positioned perpendicularly to the primary X-ray direction and very close to the sample, thus contributing to an improvement of the limits of detection compared to conventional XRF spectrometers. To perform analysis under total-reflection conditions, samples must be provided as thin films on a reflective carrier, and therefore matrix effects can be neglected. Consequently, the quantification strategy is simpler than in XRF and it can be done by adding a suitable internal standard to the sample, without the need of an empirical calibration using a set of matrix-matched standards [16].

In the last years, several research studies have been conducted using TXRF systems. For instance, TXRF was chosen as a good analytical approach for the determination of trace and sub-trace elements in micrometer thin sections of tissues, which were directly adhered on the reflective carrier as a thin film [17,18]. In other studies, TXRF analysis has been performed after an acidic digestion treatment of the biological samples. Leitão et al. [14] used HNO_3 for digesting lyophilized tissues and comparing the content of P, S, Ca, Fe, Cu, Zn, and Rb of donors with normal, malignant and benign prostate hyperplasia, while Majewska et al. [9] compared the Zn content in thyroid samples with different diseases, by digesting the samples with a mixture of high-purity HNO_3 and 30% H_2O_2. More recently, some studies have shown the potential of TXRF for the analysis of small amounts of powdered solid samples by preparing a suspension or slurry. This strategy has been applied for the analysis of biological samples such as vegetal foodstuff [19] and placenta human samples [15]. However, it is not trivial to obtain reliable results using this simple sample treatment approach and some studies reported the necessity to use more sophisticated quantification approaches to obtain reliable results [19].

In this work, we evaluate the quality of the results obtained when using suspension preparation for TXRF analysis of different types of human tissues including colon, heart, liver, lung, muscle, intestine, skin, stomach, uterus, bladder, and aorta. Although not usually discussed in literature, the analytical approach to the analysis of human tissues is usually tackled regardless of the type of organ and its characteristics, such as fat content. However, this must also be a factor to be considered when choosing the appropriate methodology, as the accuracy and precision of the analytical results may be affected. As such TXRF analysis of the same tissues but after a previous digestion of the sample was performed, and the obtained results were compared. To study the real capability of TXRF instrumentation for human tissue analysis, two TXRF systems with different anode configuration have been tested. Finally, advantages and limitations of the TXRF method have been discussed and compared with μ-EDXRF and ICP-OES analysis.

2. Materials and methods

2.1. Reagents and materials

Stock solutions of 1000 mg/L (ROMIL PrimAg@ Monocomponent reference solutions) were used to prepare Ga internal standard solutions. Ultrapure de-ionized water for preparation of sample suspensions, dilution of stock solutions and microwave digested samples was obtained from a Milli-Q purifier system (Millipore Corp., Bedford, Massachusetts). TritonTM X-100 (laboratory grade, Sigma-Aldrich) was used for the preparation of sample suspensions. Nitric acid (69%, HIPERPUR, Panreac), hydrogen peroxide solution (P30%, TraceSELECT, Sigma-Aldrich) and hydrochloric acid (37%, Panreac, AppliChem) were used for the microwave digestion procedure. Silicone solution in isopropanol (Serva, GmbH & Co, Germany) was used to coat all the quartz glass disc reflectors in order to obtain a hydrophobic film so as to facilitate sample deposition.

Different biological certified reference materials (CRMs) were employed to study the suitability of the proposed analytical methods for multi-elemental analysis: BCR-184 (Bovine muscle), BCR-185r (Bovine liver), BCR-186 (Pig kidney), NIST 1577a (Bovine liver) and NIST 1566b (Oyster tissue).

2.2. Human tissue samples and pre-treatment

Samples were collected from a deceased patient donated through the Corpses Donation Office at the Department of Anatomy of NOVA Medical School for research and educational purposes. The subject was embalmed using exclusively intra-arterial perfusion of a solution composed of aliphatic alcohols (diethylene glycol and monoethylene glycol), and then was kept in refrigerated cameras at 4 °C, with no further exposition to other fixatives or preservative alcohols, to ensure tissue preservation over time [20]. The collected tissue samples include liver, stomach, aorta, bladder, heart, uterus, skin, muscle, lung, small intestine, and ascending colon.

Samples were lyophilized using a Modulyo Freeze Dryer system (Edwards, UK) operated at −60 °C and 20 Pa for two days. The lyophilized samples were powdered in a mechanical mill and in a pestle and mortar. In Fig. 1, a scheme of the human tissue samples' treatment procedures and analytical techniques tested is shown. In the next sections specific experimental details about sample preparation, analysis and quantification using TXRF, μ-EDXRF and ICP-OES are described.

2.3. Total reflection X-ray fluorescence (TXRF) analysis

2.3.1. Sample treatment

2.3.1.1. Suspension preparation. A preliminary study was performed to select the most suitable disperser agent to suspend the biological samples. According to the obtained results (see Section 3.1.1 for details), the final sample suspensions were prepared by weighing 20 mg of sample and adding 1 mL of 2 M nitric acid containing 10 μg of Ga as internal standard. Triplicates were prepared for each sample and 15 min sonication in ultrasonic bath was applied. After that, 10 μL of the internal standardized sample was deposited on a quartz glass reflector and dried using a hot plate (80 °C) for the subsequent TXRF analysis.

2.3.1.2. Microwave digestion. A microwave acid digestion was employed for the preparation of the biological samples. About of 200 mg of sample was added to a PTFE vessel with 5 mL of nitric acid and 1 mL of hydrogen peroxide. The vessels were capped and heated following a three-stage microwave digestion program using an Ethos Plus Milestone microwave with an HPR-1000/10S high pressure rotor (Sorisole, Bergamo, Italy): Step-1) 10 min to reach 170 °C; Step-2) 15 min to reach 200 °C; and Step-3) 10 min to reach 50 °C. After cooling, the digested sample solutions were transferred to a 25 mL flask and brought to volume with ultrapure deionized water. From each sample digest, an aliquot of 1 mL was fortified with a suitable volume of a Ga solution (internal standard) to have a final concentration of 10 mg/L. The sample deposition volume and drying mode to perform TXRF analysis were the same as for the suspended samples.

2.3.2. Instrumentation

TXRF analysis of suspended and digested samples was performed using a benchtop TXRF system (S2 PICOFOX, Bruker Nano GmbH, Berlin, Germany) equipped with a 50 W X-ray tube with a tungsten (W) anode and multilayer monochromator (35.0 keV). The characteristic radiation emitted by the elements present in the sample is detected by a silicon drift detector with a resolution of 146 eV (Mn-Kα). The measurements were performed working at 50 kV and 1000 μA for 2000 s.

For comparison purposes, digested samples were also analyzed using the same TXRF system but equipped with a 50 W Mo-anode X-ray tube (S2 PICOFOX, Bruker Nano GmbH, Berlin, Germany) and multilayer monochromator for 17.5 keV. The measurements were performed working at 50 kV and 600 μA for 2000 s.

2.3.3. Quantification

As mentioned in the introduction, TXRF quantification is usually carried out by internal standardization. This method is based on the addition of an element, the internal standard (IS), which is not present in the sample. Then, element concentrations are estimated using Eq. (1):

$$C_i = \frac{N_i \times C_{IS} \times S_{IS}}{N_{IS} \times S_i} \quad (1)$$

where C_i is the analyte concentration; N_i is analyte net peak area; C_{IS} is the IS concentration; S_{IS} is the instrumental sensitivity for the IS; N_{IS} is the IS net peak area; and S_i is the instrumental sensitivity for the analyte.

This approach is only valid if the sample is presented as a thin layer on the carrier. However, in many cases, the resulting spot on the reflector is too thick to ensure the conditions of total reflection and matrix effects cannot be considered negligible, which is the premise for a proper use of internal standardization. In such cases, external calibration using a set of calibration standards can be used as a quantification approach alternative [16]. In the present work, internal standardization using Ga as IS was evaluated as a quantification approach for the determination of P, S, K, Ca, Fe, Zn and Br the target human tissue samples.

Detection limits (DL) were estimated using the 3σ approach [16].

2.4. Micro energy dispersive X-ray fluorescence (μ-EDXRF) analysis

2.4.1. Sample treatment

Human tissues powder (~ 1 g) was pressed into 15 mm diameter and 1 mm thick pellets, glued (heptane mixture) onto a Mylar film and

Table 1
Results obtained for the determination of S, K, Ca, Mn, Fe, Cu and Zn in the certified reference material SRM 1566b (Oyster tissue) using ICP-OES and μ-EDXRF methods. Results are expressed as mean concentration values of three replicates with the associated standard deviation (in mg/kg).

Element	NIST 1566b – Oyster tissue		
	Certified	*ICP-OES*	*μ-EDXRF*
S	6890 ± 140	7410 ± 80	7700 ± 1000
K	6520 ± 90	6630 ± 90	7600 ± 250
Ca	838 ± 20	756 ± 6	720 ± 50
Fe	205.8 ± 6.8	210 ± 6	300 ± 30
Cu	71.6 ± 1.6	78 ± 2	90 ± 20
Zn	1424 ± 46	1600 ± 20	1900 ± 250

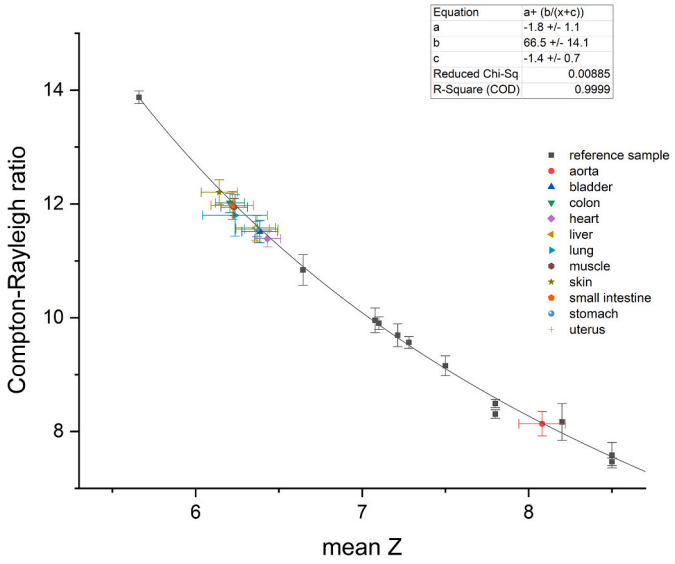

Fig. 2. Plot of the Compton to Rayleigh scattering peaks ratio as a function of the sample's mean Z determined for a set of model (reference) samples [7] and for the tissues under study.

placed on a sample holder.

2.4.2. Instrumentation

The μ-EDXRF system used was the M4 Tornado (Bruker, Germany). The X-ray tube is a micro-focus side window low-power Rh tube. A polycapillary lens was used to obtain a spot size down to 25 μm for Mo-Kα. Detection of fluorescence radiation was performed by a silicon drift detector with 30 mm^2 sensitive area and energy resolution of 142 eV for Mn-Kα. To ensure representative evaluation of the composition, instead of spot analysis, area acquisition was performed, and the accumulated spectrum was evaluated. Mappings were performed in 3 different 6 × 6 mm^2 areas, using a step size of 35 μm and time per step of 12 ms/pixel over 1 cycle, rendering a total acquisition time of 300 s. At the output of the X-ray tube, different filter combinations were used to promote the detection of light elements ($Z < 20$), 100 μm Al, and of heavier elements ($Z > 20$), 100 μm Al, 50 μm Ti, and 25 μm Cu. The X-ray tube was operated at 50 kV and the current was set at 300 μA when using the Al filter, and at 400 μA when using the Al/Ti/Cu filters combination.

2.4.3. Quantification

μ-EDXRF quantification was performed using the external calibration approach. It relies on calibration curves of the concentration of a given element as a function of the Kα peak integral divided by the scattering peaks ratio, built using a set of 15 animal and plant certified reference materials. More specific details of the calibration curves and DLs can be found in a previous publication by Machado et al. [7]. All powder CRMs were analyzed as pellets, prepared following the procedure described in Section 2.4.1.

The obtained spectra were evaluated using the advanced spectra processing tools of ROOT [21]: a fit function composed of a sum of Gaussian functions was fitted to each spectrum by χ^2 minimization techniques.

Table 1 presents the validation of the quantitative results obtained using the μ-EDXRF method for the analysis of the biological reference material NIST-1566b (Oyster tissue). As can be seen, with the exception of Fe and Zn, that are a little overestimated, there is a good agreement between the certified and the obtained values for this reference material (bias below 25%). Note that with this quantification approach, it was also possible to determine the concentration of uncertified elements, namely P and Br.

2.4.4. Mean Z determination of the samples

In order to evaluate the mean-Z values of the analyzed samples, the Compton-to-Rayleigh scattering peaks ratio was determined for the EDXRF spectra and plotted against the mean-Z model determined in Machado et al. [7]. This model was developed using a set of samples consisting of different proportions of reference materials of HAp [$Ca_{10}(PO_4)_6(OH)_2$] and boric acid [H_3BO_3] and also a paraffin block in order to obtain an average atomic number range of $5 < Z < 14$. The list of model (reference) samples with corresponding mean Z is presented in Pessanha et al. [22]. Fig. 2 depicts the obtained plot for model samples and for the analyzed human tissue samples. The mathematical fit of this dependence allowed to determine the mean Z of the real tissue samples. As can be seen, the typical human tissue has a mean Z between 6.14 (skin) and 6.43 (heart). With this information we can infer that skin have the highest amount of adipose tissue, followed by colon and intestine, while the heart had the lowest, followed by bladder and uterus. Aorta presented an extremely high mean Z, 8.08, allowing us to infer that the sample's matrix is not solely composed of a combination of H, C, O and N [23].

2.5. Inductively couple plasma optical emission spectrometry (ICP-OES) analysis

2.5.1. Sample treatment

The same microwave acid digestion method employed for the analysis of biological samples by TXRF was used (Section 2.3.1) for ICP-OES analysis. After cooling, the digested sample solutions were transferred to a 25 mL flask, brought to volume with ultrapure deionized water and analyzed by ICP-OES.

2.5.2. Instrumentation

An Agilent ICP-OES 5100 Synchronous Vertical Dual View (SVDV) spectrometer was used.

for elemental determination in digested biological samples. The following element wavelengths (nm) were employed: P (213.618), S (181.972), K (769.897), Ca (315.887), Cu (327.395), Fe (259.940), Cu (324.754), and Zn (213.857). The plasma was operated with 12 L/min plasma gas, and a silicon based multichannel array CCD (charge coupled device) detector was used. Other parameters were: 1200 W RF power, concentric nebulizer type and polychromatic wavelength selector.

2.5.3. Quantification

Empirical calibrations using a set of aqueous multielemental standards containing the analytes of interest (P, S, Ca, Cu, Fe, Cu, and Zn) were employed. To avoid matrix effects, calibration standards were prepared using an acidic solution with a matrix similar to that of the digested biological samples. Table 1 shows the results obtained for the reference material NIST-1566b (Oyster tissue) using the ICP-OES method. Considering the high accuracy of the ICP-OES method, these values were used as reference values in the case of unknown human tissue samples.

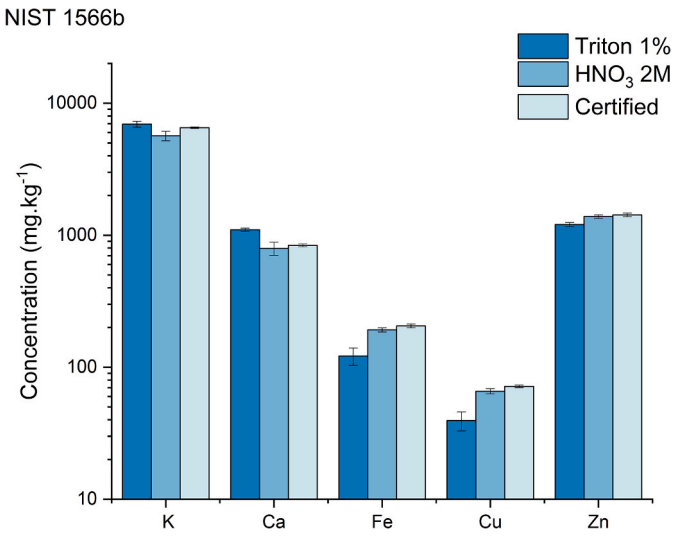

Fig. 3. Effect of the type of disperser agent on element concentration determined in the analysis of NIST 1566b: Oyster tissue reference material by suspension preparation and TXRF analyses. Results are expressed as mean concentration values with the associated standard deviation ($n = 3$). Values for other CRM can be found in supplementary material S2.

3. Results and discussion

3.1. Evaluation of analytical capabilities of TXRF for human tissues analysis

To study the real capability of TXRF for human tissues analysis, different sample treatment strategies and TXRF setups were evaluated.

3.1.1. Sample treatment procedure strategy

As mentioned in the introduction section, one of the benefits of TXRF in the analysis of solid samples is the possibility to analyze them directly by suspending a small amount of the powdered sample in an adequate disperser agent. Usually, diluted aqueous suspensions of non-ionic surfactants (e.g., Triton X-100®) are used for such purpose [24,25].

In a first set of experiments, several biological certified reference materials with different matrices (BCR-184 and NIST-1577a Bovine liver, BCR-184 Bovine muscle, BCR-186 Pig kidney, NIST-1566b Oyster tissue) were prepared as suspensions (20 mg of the powdered material in 1 mL of an aqueous solution of 1% Triton X-100) and measured by TXRF (W X-ray tube). As it is shown in Fig. 3 and supplementary material Fig. S2 (Appendix) in most cases, an underestimation of the analytes concentrations was found using this analytical approach. The only exception were the results obtained for Ca, which were significantly higher in comparison with the certified values. From the obtained results it was clear that the use of an aqueous solution of 1% Triton X-100 was not a good strategy to be used to suspend the target biological materials, possibly due to an uneven tissue deposition on the sample carrier in relation to the distribution of the internal standard. As the internal standard does not penetrate the tissue particles but only on their surface

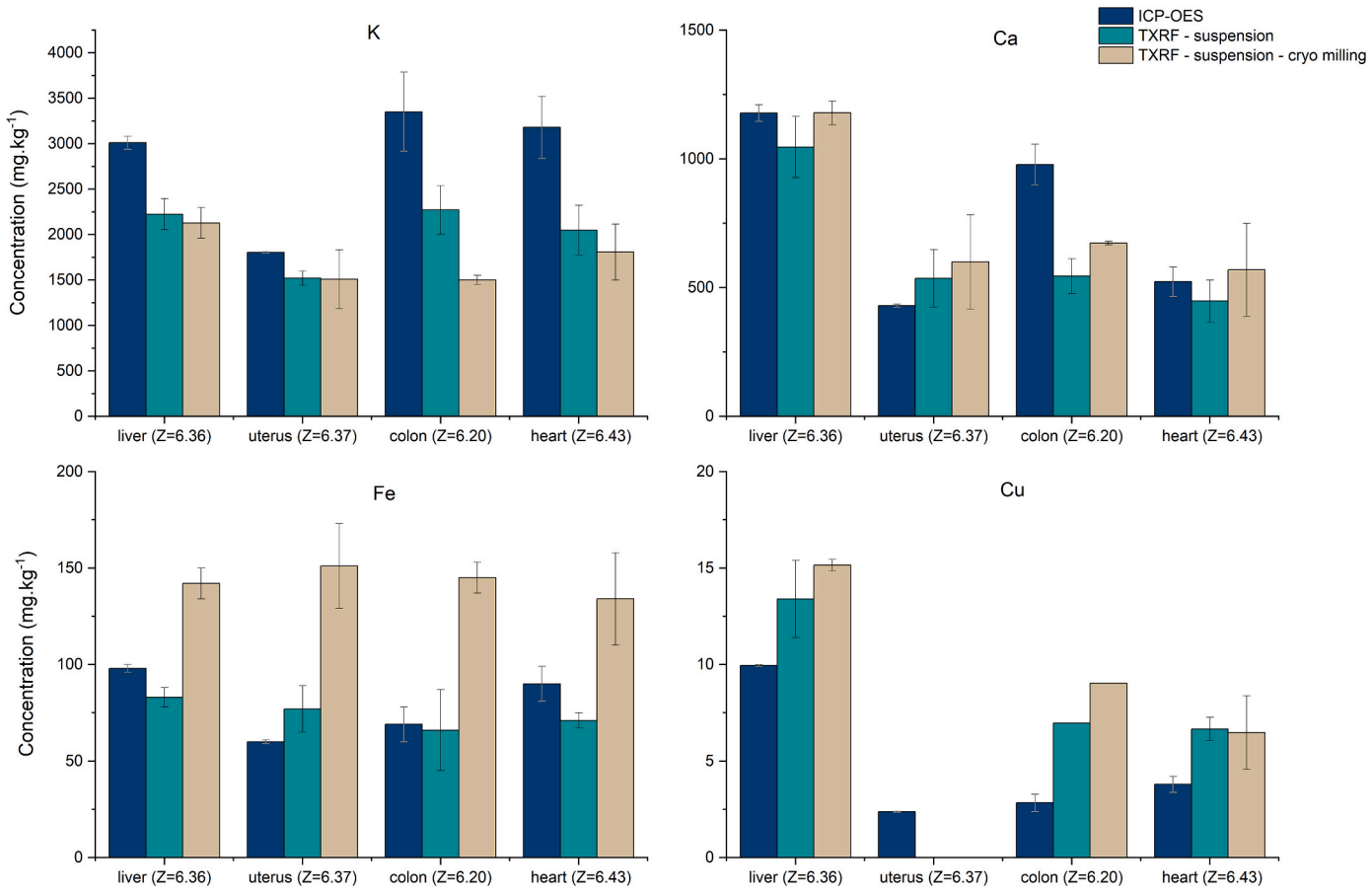

Fig. 4. Effect of cryo-milling on element concentrations determined in the analysis of human tissue samples by suspension preparation and TXRF analysis. Results are expressed as mean concentration values with the associated standard deviation (n = 3). Between brackets information about the mean Z values of the analyzed human tissue samples (see Fig. 2).

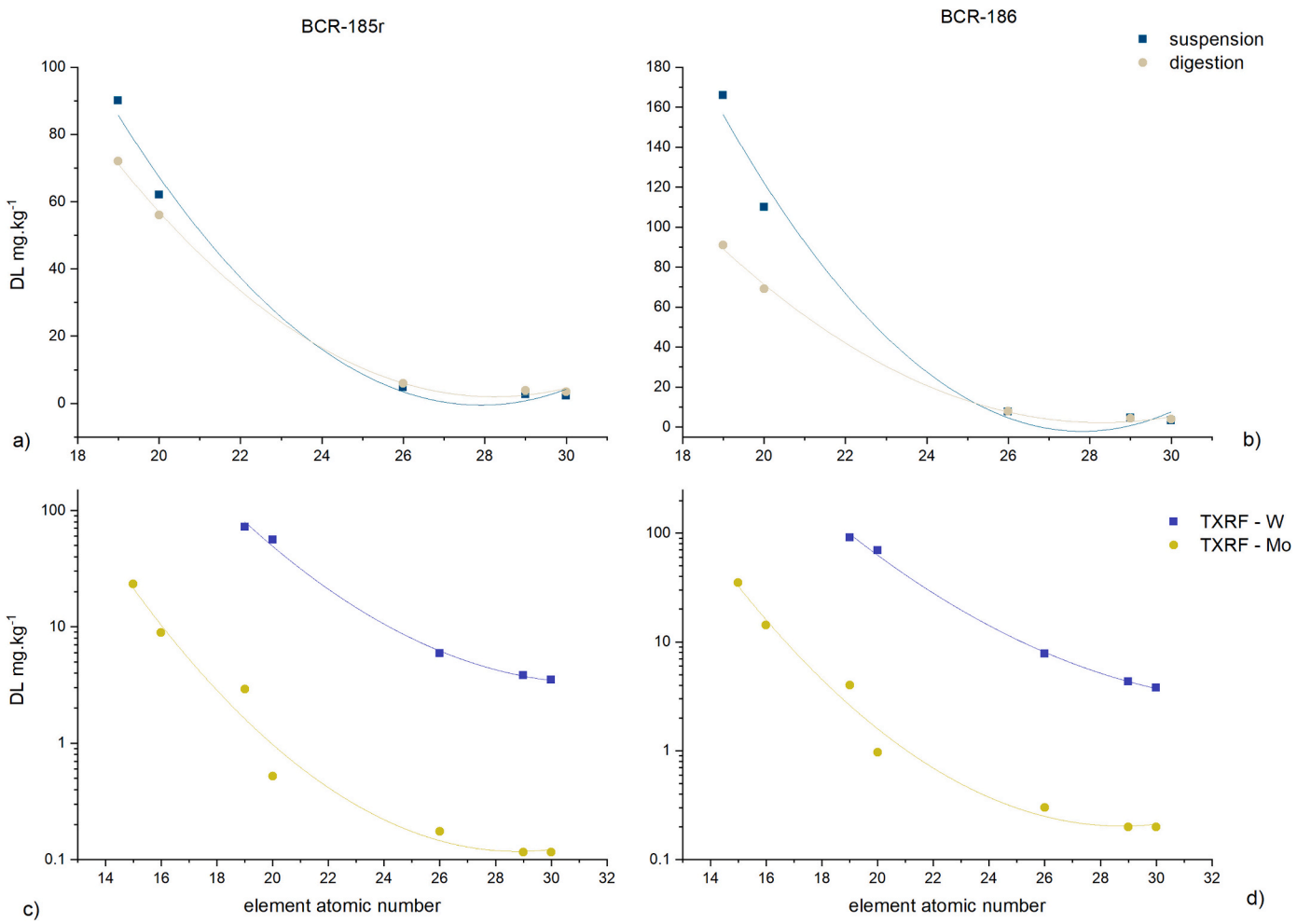

Fig. 5. Detection limits (in mg/kg) of suspension and digestion TXRF (W-anode X-ray tube) methods for the analysis of the reference materials a) Bovine liver (BCR-185r) and b) Pig kidney (BCR-186). Detection limits (in mg/kg) of TXRF W-anode and TXRF Mo-anode for the analysis of the reference materials c) Bovine liver (BCR-185r) and d) Pig kidney (BCR-186).

and in the aqueous solution, its use for quantifications purposes is no longer valid. In a previous publication, we demonstrated that when using ultrapure water or an aqueous solution of a non-ionic surfactant, the residue deposited on the quartz reflector was not homogenous and tissue particles could be seen by optical microscope analysis [26].

In view of these findings, in the present work, the reference materials were also prepared by suspending the same amount of powder in 1 mL of a diluted acidic solution (2 M HNO_3). Results displayed in Fig. 3 and Fig. S1 (Appendix) demonstrated that, in most cases, a good agreement was obtained between TXRF results and certified values when using 2 M HNO_3 as the disperser agent. This improvement can be explained by taking into account the better homogeneity of the suspension as well as the better deposition of the residue and the internal standard on the reflector using a solution of 2 M HNO_3 instead of a solution of 1% Triton X-100 (see Fig. S1). A similar finding has been recently reported by Hauser and co-workers who obtained quantitative TXRF results for placenta analysis by suspending 10 mg of powdered material in 1 mL of nitric acid [27].

After verifying the quality of the TXRF results obtained in the analysis of the aforementioned biological certified reference materials, the same analytical approach was applied for the analysis of different types of real human tissues. It is interesting to mention that in the case of some unknown samples (e.g., skin, and intestine) it was not easy to obtain a fine powder to prepare the suspension, surely due to the high adipose (fat) content, corroborated by the low mean Z value. These types of tissues are difficult to be ground to small particle sizes at ambient temperatures and so, cryomilling (performed at N_2 liquid temperature) was tested to increase the efficiency of the milling process. The extremely low milling temperature leads to finer grain structures and thus more homogeneous solid suspensions. In Fig. 4, the effect of cryo-milling on element concentrations determined in the analysis of human tissue samples by suspension preparation and TXRF analysis is shown. For comparison purposes, results obtained by digestion and ICP-OES analysis are also included as reference values. As it can be seen, in spite of obtaining a finer powder and a more homogeneous suspension, cryo-milling do not improve the quality of the analytical results (Fig. 4). Moreover, due to the use of stainless-steel grinding bowls in the cryo-milling procedure, a clear contamination of Fe content in the human tissues was found.

It is also important to remark that the quantification of low Z elements such as K by suspension preparation and TXRF analysis is hampered by absorption issues, as it has already been pointed in previous publications [19,28]. For these elements, external calibration using a set of matrix-matched standards is usually necessary to compensate the absorption effects and to improve TXRF results, which are systematically underestimated. Finally, results obtained in the determination of elements present at lower concentrations such as Cu (< 10 mg/kg) using suspension and TXRF presented low accuracy (Fig. 4), probably due to the proximity of the determined concentrations to the detection limit of the experimental setup. In view of these premises and in an attempt to improve the quality of the results obtained in the analysis of human tissues by TXRF, digestion of the samples was

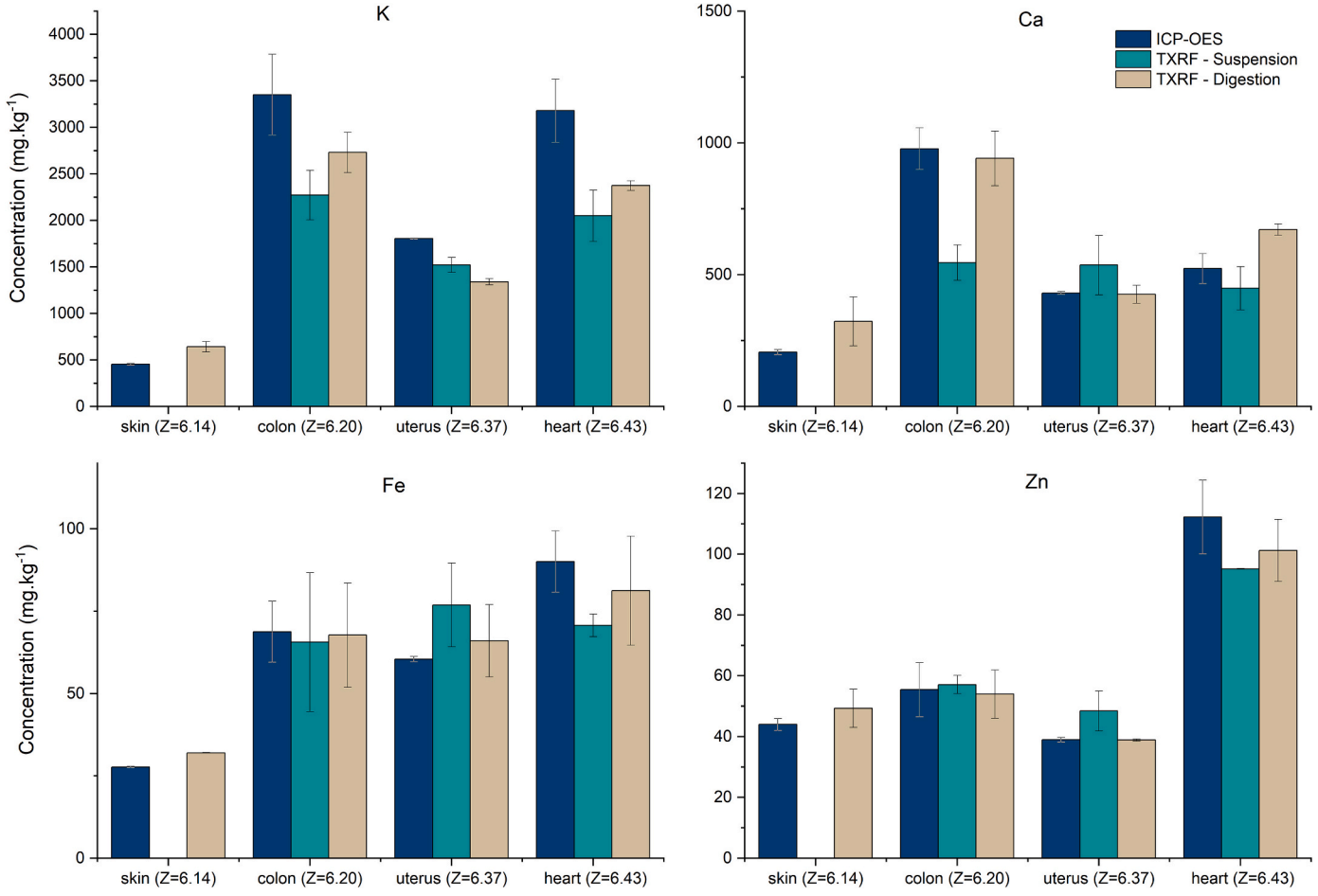

Fig. 6. Effect of sample preparation (suspension, digestion) on element concentrations determined in the analysis of human tissue samples by TXRF. Results are expressed as mean concentration values with the associated standard deviation (n = 3). Between brackets information about the mean Z values of the analyzed human tissue samples (see Fig. 2).

considered as an alternative sample preparation procedure (for details of the digestion process see Section 2.3.1). In Fig. 5a and b, limits of detection (DL) for suspension and digestion TXRF (W-anode X-ray tube) methods for the analysis of bovine liver (BCR-185r) and pig kidney (BCR-186) references materials are displayed. As it is shown, a clear improvement of the DLs for low Z elements is attained when using a digestion step before the TXRF analysis. In the case of mid-Z elements, DLs are similar for both sample preparation approaches. This fact can be related with the low concentration of these elements in the biological tissues and the higher dilution factor in the case of the digestion process (Dilution factor for suspension: 20 mg/mL; dilution factor for digestion: 8 mg/mL).

In Fig. 6, elemental concentrations obtained in the analysis of several human tissues using suspension and digestion procedures before TXRF analysis are displayed. As it can be seen, for some human tissues a clear improvement of the results is obtained when digestion is used as sample treatment (e.g., colon) and for other tissues (e.g., skin) digestion is the only sample treatment procedure that can be used. Again, this fact can be related with the fat content of the tissue.

Mean-Z values of the analyzed human tissue samples estimated by the Compton-to-Rayleigh scattering peaks ratio (μ-EDXRF spectra) are also displayed in Fig. 6. As can be seen in Fig. 6, for samples with higher mean Z, suspension and digestion provided acceptable analytical results, while for samples with lower Z, hence, higher fat content, reliable results are only obtained when digestion is performed.

Moreover, it must be noted that the quality of the results for elements present at concentrations <10 mg/kg (e.g., Cu) was quite poor even

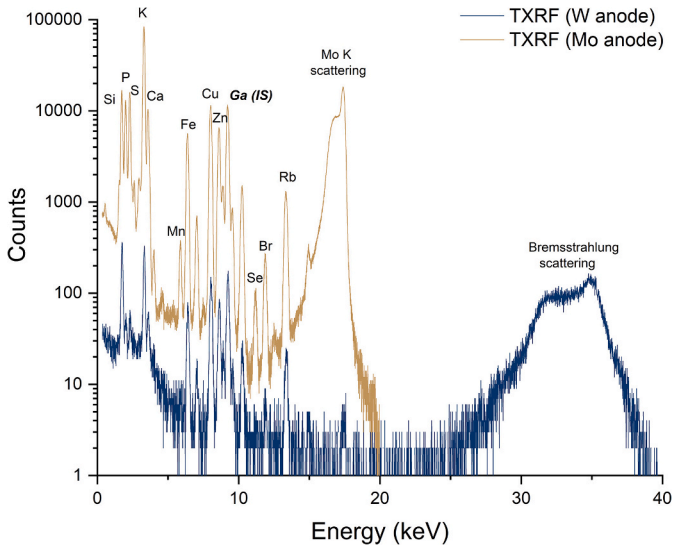

Fig. 7. TXRF spectra of characteristic radiation emitted from the sample of the reference material BCR-185r (Bovine liver) excited using primary radiation from Mo-anode and W-anode X-ray tubes.

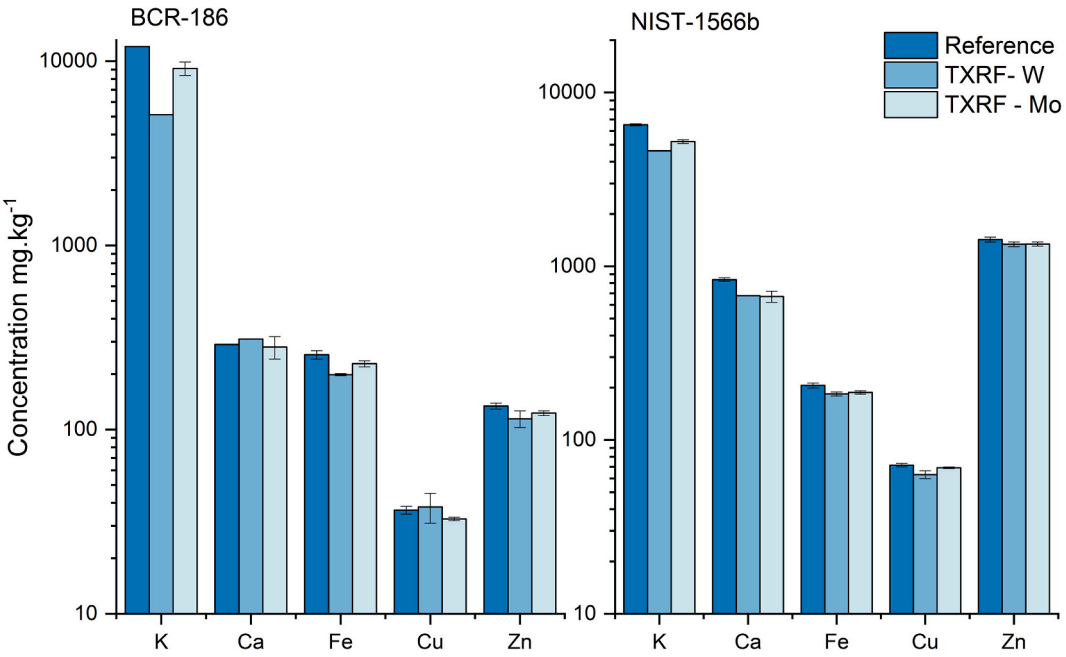

Fig. 8. Comparison of the results obtained by both TXRF systems (Mo-anode and W-anode X-ray tubes) by analyzing the reference materials BCR-186 (Pig kidney) and NIST 1566b (Oyster tissue). Results are expressed as mean concentration values with the associated standard deviation (n = 3). Values for other CRM can be found in supplementary material Fig.S3 (Appendix).

when using digestion as sample treatment strategy. Thus, to improve LD for the determination of elements present in the low mg/kg range, the analytical capabilities of another TXRF system equipped with a Mo-anode X-ray tube were explored (see Section 3.1.2).

3.1.2. *Comparison of TXRF systems equipped with W-anode and Mo-anode X-ray tubes*

TXRF spectra of characteristic radiation emitted from the sample of digested reference material BCR-185r (Bovine liver) excited using Mo-anode and W-anode X-ray tubes TXRF systems are shown in Fig. 7. In both TXRF spectra, Si lines from the quartz glass sample carrier and Ga lines (used as an internal standard, IS) are observed. In the Mo TXRF spectrum, a high intensity peaks around 17 keV are present, being a result of elastic (Rayleigh) and inelastic (Compton) scattering of the characteristic Mo Kα line of the radiation source used for excitation of the sample. In contrast, a bremsstrahlung continuum radiation is produced when a W target is used to generate X-rays. Moreover, the main differences between Mo-anode and W-anode X-ray tubes excitation, lie in the measurement energy (keV) range and the resulting TXRF signal, as evidenced by the plotted spectra (Fig. 7). In the case of the W-anode X-ray tube system, it is possible to determine elements with Z ranging from 40 to 51 through the corresponding K-lines (characteristic X-ray energy in the range from about 15 keV to 26 keV). On the other hand, the Mo-anode X-ray tube TXRF system presents a much higher sensitivity for mid-Z and low-Z elements. Even phosphorous and sulphur can be identified and quantified in the biological tissues, which was impossible with excitation using W-anode X-ray tube, as it presents a much lower photoelectric absorption cross-section for these elements. Due to the multielemental capability of TXRF, the detection of uncertified elements other than the ones discussed in this paper and present in the bovine liver sample was also possible, namely Se, Br, and Rb.

In Fig. 5c and d, detection limits for both TXRF systems, estimated by analyzing the reference materials BCR-185r (bovine liver) and BCR-186 (pig kidney), are displayed. In general, results show that DLs for presented low-mid Z (Z = 15–30) elements detected through K-alpha transitions were more than one order of magnitude lower when using the Mo-TXRF system. A slight difference between the DLs estimated in the analyzed biological tissues (BCR-185R, bovine liver and BCR-186, pig kidney) was also observed, although within the same order of magnitude. In details, when comparing these two systems, the DL can be up to two orders of magnitude higher when considering calcium or lower Z elements, or between 20-fold to 35-fold higher for transition metals.

A comparison of the results obtained for both TXRF systems (Mo-anode and W-anode X-ray tubes) in the analysis of different biological certified reference materials is presented in Fig. 8. As expected, the use of the Mo-TXRF system yields more accurate results for the determination of low Z elements (K, Ca) and elements present at low concentrations (Cu). For other mid-Z elements results were similar using both TXRF instruments.

3.2. *Application of TXRF for real human tissue analysis and comparison with μ-EDXRF and ICP-OES*

Finally, results obtained using the determined best conditions for the TXRF analysis of human tissue samples (digestion + Mo-anode X-ray tube excitation) were compared with those obtained by μ-EDXRF and ICP-OES. Results for some of the analyzed tissues are presented in Fig. 9 and in supplementary material Fig. S4 (Appendix).

In most cases, TXRF results were comparable to those obtained by ICP-OES, except for Sulphur, whose calculated concentration values were found to be systematically lower. Nevertheless, as it is shown in Table 1, recovery value for Sulphur determination when using ICP-OES analysis for the reference material NIST 1566b (Oyster tissue) was slightly over estimated (R ~ 108%, certified: 6890 ± 140 mg/kg, ICP-OES: 7410 ± 80 mg/kg).

TXRF method provides better results than μ-EDXRF, in terms of accuracy and precision, for the quantification of elements present at concentration levels lower than 10 mg/kg. A significant additional advantage of TXRF over μ-EDXRF is the possibility to use internal standardization as a quantification approach and therefore, empirical calibration using a set of biological reference materials is not required. Nevertheless, to obtain reliable results for multielemental analysis of human tissue samples, a previous sample treatment to destroy the organic matrix and the fat content by means of a digestion procedure is needed in the case of TXRF.

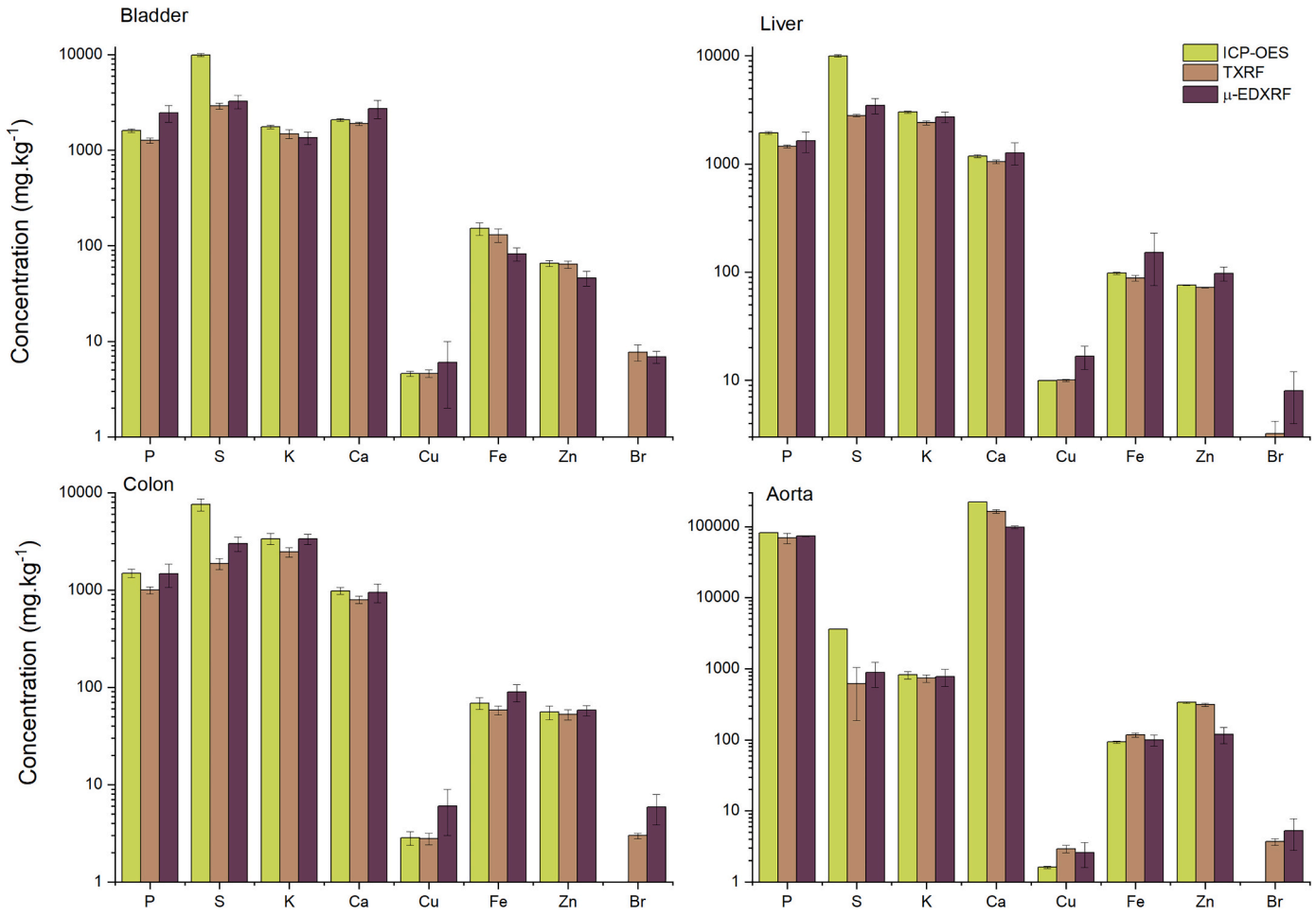

Fig. 9. Comparison of the results obtained in the determination of P, S, K, Ca, Cu, Fe and Zn in Bladder, Liver, Colon and Aorta samples using TXRF, ICP-OES and μ-EDXRF methods. Results are expressed as mean concentration values of three replicates with the associated standard deviation (in mg/kg). Values for other tissues can be found in supplementary material S4.

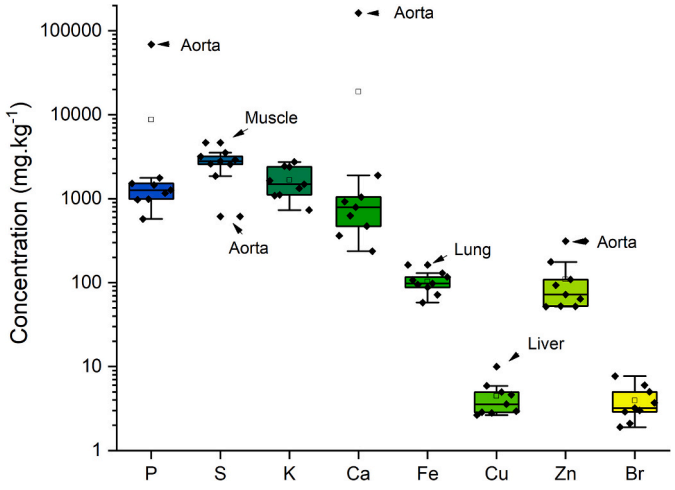

Fig. 10. Box-whiskers plot of the concentration distributions obtained for P, S, K, Ca, Cu, Fe and Zn, for all the tissues, determined using TXRF instrumentation. The box (interquartile range (from 25th to 75th percentiles)) overlaps with the data in order to gauge distribution. Open squares represent the mean value of element concentration, black line in each box represents median while whiskers are ranges from 10th to 90th percentiles.

On the other hand, EDXRF can be applied directly to the sample or pelletized sample without another sample preparation. This makes this technique suitable for the analysis of Formalin Fixed Paraffin Embedded, stored in hospitals after biopsies [29].

It should also be noted that bromine was not determined by ICP-OES, and the values obtained by μ-EDXRF are consistently higher than for TXRF. The former may present greater deviations from the actual concentration values as we had a limited number of CRMs with certified Br concentration values (yielding a calibration curve with few points). Moreover, in most CRMs the element is present in trace amounts, further hindering quantification.

In view of the obtained results, future studies should be focused on the optimization of the sample preparation process, particularly the digestion of human tissues, for a more sustainable TXRF analysis. Considering the analytical capability of TXRF, a miniaturized digestion process could be tested, so that the amount of sample and reagents could be reduced, and limits of detection improved (lower dilution factor).

3.3. *Comparison of the obtained results with literature*

Regarding the quantitative results obtained for the real samples (Fig. 10) they are also well aligned with the elemental concentrations found in literature (Table 2). Although research studies are mainly focused on breast, colon, and prostate, most likely due to the higher incidence of cancer in these organs, some comparisons can still be performed. With the exception of the aorta sample, that presented an elevated amount of P and Ca (7 ± 1 *w*/w% and 16 ± 1 w/w%,

Table 2
Overview of the elemental concentration ranges (in mg/kg) found in literature for different human tissue samples.

	P	S	K	Ca	Fe	Cu	Zn	Br
Lung	967 ± 58 [31] to 29,700 ± 810 [18]	1326 ± 68 [31] to 3030 ± 1080 [18]	64 ± 13 [18] to 253 ± 17 [31]	660 ± 270 [18] to 2470 ± 450 [31]	75.1 ± 9.66 [31] to 316 ± 140 [18]	2.71 ± 0.175 [31]	11.6 ± 0.492 [31] to 21 ± 7 [18]	
Liver					134–2550 [32]	7.3–56 [32]	24–591 [32]	
Uterus	2210 ± 120 [18]	3775 ± 280 [18]	571 ± 50 [18]	1590 ± 90 [18]	59 ± 6 [18]	4 ± 1 [18]	40 ± 3 [18]	
Colon	420 to 1980 [17]	2370 ± 620 to 5110 ± 850 [18]	454 ± 155 to 1830 ± 430 [18]	465 ± 47 to 1340 ± 480 [18]	51 ± 23 to 150 ± 45 [18]	5 ± 2 to 13 ± 4 [18]	33 ± 10 to 83 ± 9 [18]	2.0 ± 0.5 to 7 ± 1 [18] 3 ± 1 to 9 ± 1 [18]
Stomach			387 ± 62 [33]	647 ± 32 [33]	2408 ± 96 [33]	63.5 ± 9.4 [33]	818 ± 41 [33]	
Aorta				1026 ± 757 [30]	28.7 ± 11.7 [30]	1.3 ± 0.4 [30]	19.8 ± 4.2 [30]	
Other tissues	1000 to 8240 [34]	295 ± 120 [18] to 10,756 ± 1587 [35]	17 ± 8 [18] to 6418 ± 2625 [36]	153 ± 53 [18] to 2715 ± 1207 [35]	5 ± 2 [18] to 223 ± 95 [36]	2 ± 1 to 35 ± 5 [18]	6 ± 3 [18] to 699 ± 221 [35]	9.8 ± 4.6 [33]

respectively) most likely due to the presence of calcifications, the values found for these elements, for the remaining tissues, are within the expected concentrations. Phosphorus value in the small intestine sample (570 ± 30 mg/kg) is also below the range presented in Table 2 for other tissues, however, there is a lack of literature to compare and evaluate the meaning of this result. Sulphur values are also very similar between tissues, with a higher average value determined for the Muscle sample (4600 ± 340 mg/kg) and a lower value present in Aorta (600 ± 400 mg/kg). Although potassium values are found to vary the most within and between organs in literature, in what concerns the results obtained in our study, they present a regular distribution. For this element, Aorta also presents the lower average concentration (730 ± 80 mg/kg). Iron also presented a small range of concentrations within the tissues, with a higher value for the lung sample (160 ± 10 mg/kg), well within the values found in literature for this element in lung (Table 2). Copper and bromine are present in tissues in trace concentrations, usually below 10 $\mu g.g^{-1}$, while Zn is present in a range from 50 to 170 mg/kg, with exception of the Aorta sample where it was found in an average concentration of 310 ± 20 mg/kg, much higher than what was determined by Edvinsson et al. [30], however, the calcifications present in this tissue sample hinder any valuable comparison.

4. Conclusions

In this work, we have evaluated the potential of several analytical approaches combined with TXRF spectrometry for multielemental analysis of human tissues. An important part of the use of these methodologies is to understand and recognize their capabilities and limitations and to evaluate their suitability and complementarity depending on the objective of the analyses and on the characteristics of the biological sample.

The use of direct analysis of tissue suspensions by TXRF can be interesting as a fast and relatively simple methodology to get a first approximation of the multielemental composition of the tissue or when an extremely small amount of sample is available provided that the elemental content is sufficiently high. The main drawback of the suspension method when dealing with the analysis of human tissues is obtaining an adequate powdered sample to get a homogeneous suspension. For tissues with a high adipose content, this is very difficult and more sophisticated sample treatments such as digestion are required. A further enhancement of the limits of detection and accuracy of the results can be also achieved if using Mo-TXRF systems instead of W-TXRF instrumentation, above all for the determination of low Z elements (K, Ca) and elements present at low concentrations (Cu) in the human tissues.

In comparison with μ-EDXRF, the proposed TXRF method provides better accuracy and precision of the results for elements present at concentration levels lower than 10 mg/kg. Another significant advantage is the possibility of quantification by internal standardization without the need to use a set of biological reference materials.

Author statement

Patrícia Carvalho - Formal analysis, Data curation, Writing - original draft, Writing - review & editing.

Eva Marguí - Formal analysis, Data curation, Writing - original draft and Writing review & editing.

Aldona Kubala-Kukus - Formal analysis, Data curation and Writing - original draft.

Dariusz Banas - Formal analysis and Data curation.

Jorge Machado - Software and Writing - original draft.

José Paulo Santos – Funding acquisition and Writing - original draft.

Diogo Casal - Conceptualization and Writing - original draft.

Diogo Pais - Supervision.

Sofia Pessanha- Methodology, Writingoriginal draft and Writing - review & editing.

Declaration of Competing Interest

There are no conflicts of interest.

Data availability

Data will be made available on request.

Acknowledgments

This work was partially supported by the research centre grant UID/FIS/04559/2021 to LIBPhys-UNL from the FCT/MCTES/PIDDAC, Portugal.

Patrícia M. S. Carvalho acknowledges the support of FCT (Portugal) under contract No. PD/BD/128324/2017.

This article/publication is based upon work from COST Action CA18130 ENFORCE TXRF, supported by COST (European Cooperation

in Science and Technology, www.cost.eu).

Appendix A. Supplementary data

Supplementary data to this article can be found online at https://doi.org/10.1016/j.sab.2022.106548.

References

[1] M. Yaman, Comprehensive comparison of trace metal concentrations in cancerous and non-cancerous human tissues, Curr. Med. Chem. 13 (2006) 2513–2525, https://doi.org/10.2174/092986706778201620.

[2] A. Al-Ebraheem, K. Geraki, R. Leek, A.L. Harris, M.J. Farquharson, The use of biometal concentrations correlated with clinical prognostic factors to assess human breast tissues, X-Ray Spectrom. 42 (2013) 330–336, https://doi.org/10.1002/xrs.2463.

[3] G.R. Monteith, D. McAndrew, H.M. Faddy, S.J. Roberts-Thomson, Calcium and cancer: targeting Ca2+ transport, Nat. Rev. Cancer 7 (2007) 519–530, https://doi.org/10.1038/nrc2171.

[4] U. Majewska, D. Banaś, J. Braziewicz, S. Góźdź, A. Kubala-Kukuś, M. Kucharzewski, Trace element concentration distributions in breast, lung and colon tissues, Phys. Med. Biol. 52 (2007) 3895–3911, https://doi.org/10.1088/0031-9155/52/13/016.

[5] A. Banas, W.M. Kwiatek, K. Banas, M. Gajda, B. Pawlicki, T. Cichocki, Correlation of concentrations of selected trace elements with Gleason grade of prostate tissues, J. Biol. Inorg. Chem. 15 (2010) 1147–1155, https://doi.org/10.1007/s00775-010-0675-5.

[6] P.M.S. Carvalho, S. Pessanha, J. Machado, A.L. Silva, J. Veloso, D. Casal, D. Pais, J. P. Santos, Energy dispersive X-ray fluorescence quantitative analysis of biological samples with the external standard method, Spectrochim. Acta B Atomic Spectrosc. 174 (2020), https://doi.org/10.1016/j.sab.2020.105991.

[7] J. Machado, P.M. Carvalho, A. Félix, D. Doutel, J.P. Santos, M.L. Carvalho, S. Pessanha, Accuracy improvement in XRF analysis for the quantification of elements ranging from tenths to thousands μg g −1 in human tissues using different matrix reference materials, J. Anal. At. Spectrom. 35 (2020) 2920–2927, https://doi.org/10.1039/d0ja00307g.

[8] M.P. Silva, D.F. Soave, A. Ribeiro-silva, M.E. Poletti, Trace elements as tumor biomarkers and prognostic factors in breast cancer : a study through energy dispersive x-ray fluorescence, BMC Res Notes 5 (2012) 194–205.

[9] U. Majewska, J. Braziewicz, D. Banaś, A. Kubala-Kukuś, M. Kucharzewski, J. Waler, S. Góźdź, J. Wudarczyk, Zn Concentration in Thyroid Tissue and Whole Blood of Women with Different Diseases of Thyroid, 2001.

[10] P.M. Wróbel, S. Bała, M. Czyzycki, M. Golasik, T. Librowski, B. Ostachowicz, W. Piekoszewski, A. Surówka, M. Lankosz, Combined micro-XRF and TXRF methodology for quantitative elemental imaging of tissue samples, Talanta. 162 (2017) 654–659, https://doi.org/10.1016/j.talanta.2016.10.043.

[11] A. Kubala, D. Banaś, J. Braziewicz, S. Góźdź, U. Majewska, M. Pajek, Analysis of elemental concentration censored distributions in breast malignant and breast benign neoplasm tissues, Spectrochim. Acta B At. Spectrosc. 62 (2007) 695–701, https://doi.org/10.1016/j.sab.2007.03.004.

[12] S. Zaichick, V. Zaichick, The Br, Fe, Rb, Sr, and Zn contents and interrelation in intact and morphologic normal prostate tissue of adult men investigated by energy-dispersive X-ray fluorescent analysis, X-Ray Spectrom. 40 (2011) 464–469, https://doi.org/10.1002/xrs.1370.

[13] B.Z.R. Sitko, Quantification in X-ray fluorescence spectrometry, X-ray spectroscopy, in: S.K. Sharma (Ed.), X Ray Spectroscopy, InTech Open, 2012, pp. 137–162.

[14] M. Mantler, N. Kawahara, How accurate are modern fundamental parameter methods? Rigaku J. 21 (2004) 17–25. http://www.rigaku.com/downloads/journal/online-contents.html.

[15] S. Pessanha, C.F.J.P. Santos, A.A. Dias, Comparison of Standard - Based and Standardless Methods of Quantification Used in X - Ray Fluorescence Analysis : Application to the Exoskeleton of Clams, 2018, pp. 108–115, https://doi.org/10.1002/xrs.2819.

[16] E. Margui, R. Van Grieken, X-Ray Fluorescence Spectrometry and Related Techniques: An Introduction, Momentum Press, New York, 2013.

[17] T. Magalhães, M.L. Carvalho, A. von Bohlen, M. Becker, Study on trace elements behaviour in cancerous and healthy tissues of colon, breast and stomach: Total reflection X-ray fluorescence applications, Spectrochim. Acta B At. Spectrosc. 65 (2010) 493–498, https://doi.org/10.1016/j.sab.2010.04.001.

[18] T. Magalhães, A. von Bohlen, M.L. Carvalho, M. Becker, Trace elements in human cancerous and healthy tissues from the same individual: a comparative study by TXRF and EDXRF, Spectrochim. Acta B At. Spectrosc. 61 (2006) 1185–1193, https://doi.org/10.1016/j.sab.2006.06.002.

[19] R. Dalipi, E. Marguí, L. Borgese, L.E. Depero, Multi-element analysis of vegetal foodstuff by means of low power total reflection X-ray fluorescence (TXRF) spectrometry, Food Chem. 218 (2017) 348–355, https://doi.org/10.1016/j.foodchem.2016.09.022.

[20] J. Goyri-O'neill, D. Pais, F. Freire De Andrade, P. Ribeiro, A. Belo, A. O'neill, S. Ramos, C.N. Marques, Improvement of the embalming perfusion method: the innovation and the results by light and scanning electron, Microscopy 26 (2013) 188–194. www.actamedicaportuguesa.com.

[21] I. Antcheva, M. Ballintijn, B. Bellenot, M. Biskup, R. Brun, N. Buncic, P. Canal, D. Casadei, O. Couet, V. Fine, L. Franco, G. Ganis, A. Gheata, D.G. Maline, M. Goto, J. Iwaszkiewicz, A. Kreshuk, D.M. Segura, R. Maunder, L. Moneta, A. Naumann, E. Offermann, V. Onuchin, S. Panacek, F. Rademakers, P. Russo, M. Tadel, ROOT — a C++ framework for petabyte data storage, statistical analysis and visualization, Comput. Phys. Commun. 180 (2009) 2499–2512, https://doi.org/10.1016/j.cpc.2009.08.005.

[22] S. Pessanha, S. Silva, L.S. Martins, J.P. Santos, J.M. Silveira, Suitability of Compton-to-Rayleigh ratio in X ray fluorescence spectroscopy: hydroxyapatite-based materials characterization, J. Anal. At. Spectrom. (2019), https://doi.org/10.1039/C8JA00370J.

[23] A. Ensina, P.M. Carvalho, J. Machado, M.L. Carvalho, D. Casal, D. Pais, J.P. Santos, A.A. Dias, S. Pessanha, Analysis of human tissues using energy dispersive X ray fluorescence – dark matrix determination for the application to cancer research, J. Trace Elem. Med. Biol. 68 (2021), https://doi.org/10.1016/j.jtemb.2021.126837.

[24] H. Gallardo, I. Queralt, J. Tapias, L. Candela, E. Margui, Bromine and bromide content in soils: analytical approach from total reflection X-ray fluorescence spectrometry, Chemosphere. 156 (2016) 294–301, https://doi.org/10.1016/j.chemosphere.2016.04.136.

[25] I. de La Calle, N. Cabaleiro, V. Romero, I. Lavilla, C. Bendicho, Sample pretreatment strategies for total reflection X-ray fluorescence analysis: a tutorial review, Spectrochim. Acta B At. Spectrosc. 90 (2013) 23–54, https://doi.org/10.1016/j.sab.2013.10.001.

[26] E. Marguí, P. Ricketts, H. Fletcher, A.G. Karydas, A. Migliori, J.J. Leani, M. Hidalgo, I. Queralt, M. Voutchkov, Total reflection X-ray fluorescence as a fast multielemental technique for human placenta sample analysis, Spectrochim. Acta B At. Spectrosc. 130 (2017) 53–59, https://doi.org/10.1016/j.sab.2017.02.008.

[27] S. Hauser, S. Andres, K. Leopold, Determination of trace elements in placenta by total reflection X-ray fluorescence spectrometry: effects of sampling and sample preparation, Anal. Bioanal. Chem. 414 (2022) 4519–4529, https://doi.org/10.1007/s00216-022-04112-5.

[28] F. Bilo, L. Borgese, G. Pardini, E. Marguí, A. Zacco, R. Dalipi, S. Federici, M. Bettinelli, M. Volante, E. Bontempi, L.E. Depero, Evaluation of different quantification modes for a simple and reliable determination of Pb, Zn and cd in soil suspensions by total reflection X-ray fluorescence spectrometry, J. Anal. At. Spectrom. 34 (2019) 930–939, https://doi.org/10.1039/c9ja00040b.

[29] P.M. Wróbel, Ł. Chmura, P. Kasprzyk, K. Kozlowski, K. Wątor, M. Szczerbowska-Boruchowska, Feasibility study of elemental analysis of large population of formalin fixed paraffin embedded tissue samples – preliminary results, Spectrochim. Acta B Atomic Spectrosc. 173 (2020), https://doi.org/10.1016/j.sab.2020.105971.

[30] M. Edvinsson, N.G. Ilbäck, P. Frisk, S. Thelin, C. Nyström-Rosander, Trace element changes in thoracic aortic dissection, Biol. Trace Elem. Res. 169 (2016) 159–163, https://doi.org/10.1007/s12011-015-0432-2.

[31] A. Kubala-Kuku, J. Braziewicz, D. Bana, U. Majewska, A. Urbaniak, Trace Element Load in Cancer and Normal Lung Tissue, Nuclear Instruments and methods in Physics Research 150 (1999) 193–199.

[32] M.L. Carvalho, J. Brito, M.A. Barreiros, Study of Trace Element Concentrations in Human Tissues by Spectrometry¤ EDXRF, 1998.

[33] S.B. Reddy, M.J. Charles, G.J.N. Raju, V. Vijayan, B.S. Reddy, M.R. Kumar, B. Sundareswar, Trace elemental analysis of carcinoma kidney and stomach by PIXE method, Nucl. Instrum. Methods Phys. Res., Sect. B 207 (2003) 345–355, https://doi.org/10.1016/S0168-583X(03)00463-4.

[34] A.N. Garg, V. Singh, R.G. Weginwar, V.N. Sagdeo, An elemental correlation study in cancerous and normal breast tissue with successive clinical stages by neutron activation analysis, Biol. Trace Elem. Res. 46 (1994) 185–202, https://doi.org/10.1007/BF02789296.

[35] R.G. Leitão, A. Palumbo, P.A.V.R. Souza, G.R. Pereira, C.G.L. Canellas, M.J. Anjos, L.E. Nasciutti, R.T. Lopes, Elemental concentration analysis in prostate tissues using total reflection X-ray fluorescence, Radiat. Phys. Chem. 95 (2014) 62–64, https://doi.org/10.1016/j.radphyschem.2012.12.044.

[36] V. Zaichick, S. Zaichick, Levels of chemical element contents in thyroid as potential biomarkers for cancer diagnosis (a preliminary study), J. Cancer Metastasis Treat. 2018 (2018), https://doi.org/10.20517/2394-4722.2018.52.